

## Strong and ductile nanostructured Cu-carbon nanotube composite

Hongqi Li,<sup>1,a)</sup> Amit Misra,<sup>1</sup> Zenji Horita,<sup>2</sup> Carl C. Koch,<sup>3</sup> Nathan A. Mara,<sup>4</sup> Patricia O. Dickerson,<sup>4</sup> and Yuntian Zhu<sup>3</sup>

<sup>1</sup>Center for Integrated Nanotechnologies, Los Alamos National Laboratory, Los Alamos, New Mexico 87545, USA

<sup>2</sup>Department of Materials Science and Engineering, Kyushu University, Fukuoka 819-0395 Japan

<sup>3</sup>Department of Materials Science and Engineering, North Carolina State University, Raleigh, North Carolina 27695, USA

<sup>4</sup>Materials Science and Technology Division, Los Alamos National Laboratory, Los Alamos, New Mexico 87545, USA

(Received 13 July 2009; accepted 31 July 2009; published online 21 August 2009)

Nanocrystalline carbon nanotube (CNT)—reinforced Cu composite (grain size <25 nm) with high strength and good ductility was developed. Pillar testing reveals that its strength and plastic strain could be as large as 1700 MPa and 29%, respectively. Compared with its counterpart made under the same condition, an addition of 1 wt % CNTs leads to a dramatic increase in strength, stiffness and toughness without a sacrifice in ductility. Microstructural analysis discloses that in the Cu matrix, CNTs could be distributed either at grain boundaries or inside grains and could inhibit dislocation nucleation and motion, resulting in an increase in the strength. © 2009 American Institute of Physics. [DOI: 10.1063/1.3211921]

Carbon nanotubes (CNTs) have a unique structure<sup>1</sup> and possess extraordinary mechanical properties.<sup>2–4</sup> They exhibit superhigh elastic modulus and strength and, also, own an important set of attributes such as lightweight, high aspect ratio and excellent chemical stability.<sup>2–4</sup> These exceptional properties make CNTs an ideal nanoscale reinforcement to tailor multifunctional composites with optimal properties and superior performance. Therefore, different composites reinforced by CNTs have been reported. Past research effort mainly focused on the polymer/ceramic-based CNT composites<sup>5–8</sup> and studies on metal-CNT composites are relatively limited. However, in light of potential structural applications, research interest in the CNT-metallic matrix composites has been growing rapidly for the past five years.<sup>9–21</sup> Generally, incorporating CNTs into metallic matrices can improve strength<sup>9–21</sup> and the strength may depend on the amount of CNTs added.<sup>11–13</sup> In most cases, although the effect of CNTs on microstructure was not well characterized, both low yield strength and high temperature sintering applied during fabrication suggest that these composites are coarse/ultrafine grained materials. As far as the ductility is concerned, metal-CNT composites usually have a plastic strain ranging from 1% to 15%.<sup>13–27</sup> The higher ductility is often observed in larger grained composites that have relatively low strengths.<sup>21</sup> For the purpose of advanced structural applications, high strength composites coupled with good ductility are still desired. An efficient way of improving strength is to decrease the grain size to nanocrystalline regime (<100 nm).<sup>26</sup> Nevertheless, nanostructured metal-CNT composites with a combination of high strength and good plasticity have not been reported thus far. The present study is aimed at using a unique approach of ball milling, powder consolidation and high-pressure torsion (HPT) to develop nanostructured multiwalled CNT-reinforced copper matrix composites that exhibit high strength and ductility.

The mixture of Cu powders (0.5–1.5  $\mu\text{m}$ ) and multiwalled CNTs was ball milled in an argon protected environment for 5 h. For a reliable comparison, Cu and Cu-CNT composites (1 wt % CNT) were made under the same condition. The ball-milled powders were isostatically compacted into 10 mm diameter disks, which were then consolidated using high-pressure torsion under 6 GPa for five revolutions. All these processes were performed at room temperature. The microstructure characterization was carried out using transmission electron microscopy (TEM). The focused ion beam technique was employed to prepare pillar samples, which were compressed in a Hysitron Triboindenter nanoindenter equipped with a 30  $\mu\text{m}$  diameter flat diamond head. The pillar geometries before and after compression were characterized using scanning electron microscopy (SEM).

Figure 1 shows microstructures of the HPT-processed samples with 1 and 0 wt % CNTs. It is clear that both samples have a nanocrystalline microstructure and the grain size distribution of Cu-CNT nanocomposite is apparently narrower than that of Cu. The average grain size is about 22 and 29 nm for Cu-CNT composite and Cu, respectively. The principle of producing nanostructures by HPT is to form subgrain boundaries via dislocation accumulation and rearrangements under severe shear strain. These subgrain boundaries then develop into high-angle grain boundaries, resulting in grain refinement. At the same time, dynamic recovery and recrystallization reduce the dislocation density and may increase the grain size. The balance of these two opposite processes determines the final grain size. With the incorporated CNTs, the dislocation motion could be blocked at CNT-Cu interfaces. That is, the dislocation accumulation would be enhanced. Consequently, an addition of CNTs leads to a decrease in grain size. Figure 2 displays the CNTs embedded in the Cu matrix. Figure 2(a) shows some CNTs penetrating the Cu grains. On the other hand, in Fig. 2(b), some CNTs appear to surround the Cu grains, indicating the presence of CNTs at grain boundaries. The distribution of CNTs was evaluated using microscopic TEM investigation and macro-

<sup>a)</sup>Electronic mail: hongqi2007@gmail.com.

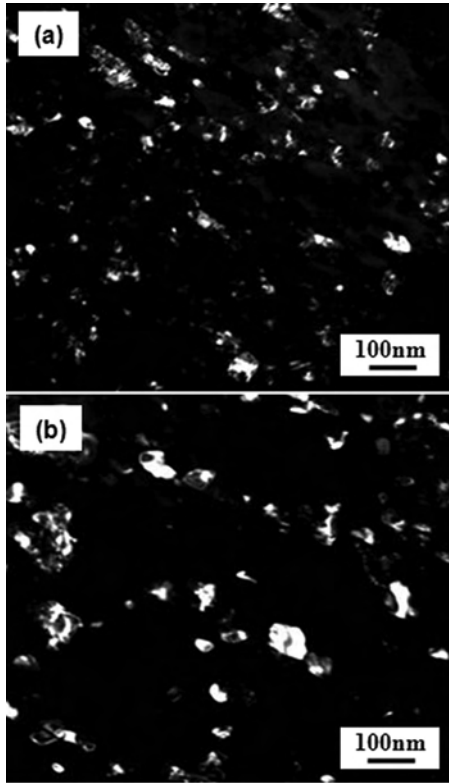


FIG. 1. Dark filed TEM micrographs of nanostructured (a) Cu-CNT composite and (b) Cu.

scopic microhardness measurement. Both results suggested that the distribution of CNTs in Cu matrix is homogeneous.

Mechanical properties of nanostructured Cu and Cu-CNT composite were investigated by pillar compression tests

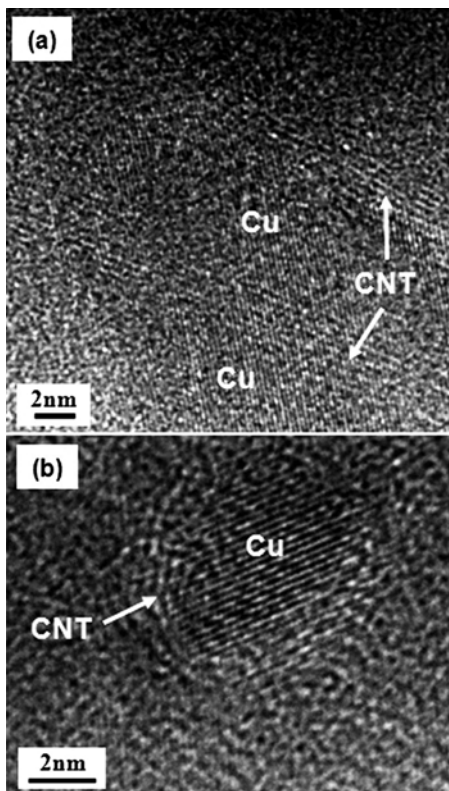


FIG. 2. High resolution TEM analysis of Cu-CNT nanocomposite.

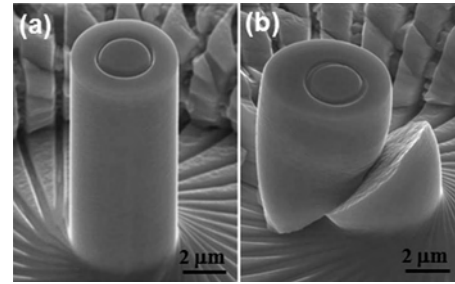


FIG. 3. SEM images of (a) an as-prepared and (b) a failed pillar samples of Cu-CNT composite.

at a strain rate of  $1 \times 10^{-3} \text{ s}^{-1}$ . Figure 3(a) presents a cylindrical pillar machined from the Cu-CNT nanocomposite. The diameter and length of all the pillars are about 5 and 11  $\mu\text{m}$ , respectively, leading to an aspect ratio of 1:2. The pillar compression technique has mostly been used to measure the effect of sample size on the strength of metallic single crystals.<sup>28</sup> In the case of nanolayered and nanostructured metals,<sup>29,30</sup> when the pillar dimension is much larger than the crystallite size, the pillar compression test can be used to study the effect of crystallite size on the strength, as opposed to the sample size. Figure 3(b) illustrates a failed sample of Cu-CNT composite, which exhibits shear instability, a typical failure mode in compression testing.

Figure 4 displays the stress-strain curves of HPT-consolidated nanostructured Cu and Cu-CNT composite. It is apparent that both samples exhibit high strength and good ductility. Calculation further finds that, on average, the yield strengths (measured at 0.2% plastic strain) are  $1125 \pm 10$  and  $738 \pm 48$  MPa and plastic strains are  $28.4\% \pm 1.9\%$  and  $30.7\% \pm 0.9\%$  for nanostructured Cu-CNT composite and Cu, respectively. In early investigations, although an addition of CNTs has been shown to increase the strength, CNT-reinforced composites either have very limited ductility or show a notable decrease in the plastic strain compared to their monolithic counterparts.<sup>13-27</sup> Interestingly, in the current study, incorporating CNTs into Cu matrix results in a great gain in strength without much sacrifice in ductility. Figure 5 summarizes the reported<sup>13-16</sup> and current compression data, where red and blue points denote maximum and yield stress data, respectively. For a comprehensive comparison, tensile data of Al-CNT,<sup>17-21</sup> AISi-CNT,<sup>22</sup> 2024Al-CNT,<sup>23</sup> Cu-CNT,<sup>24</sup> Mg-CNT,<sup>25</sup> Ni-CNT,<sup>26</sup> and AZ91D-CNT (Ref. 27) composites are also included. In gen-

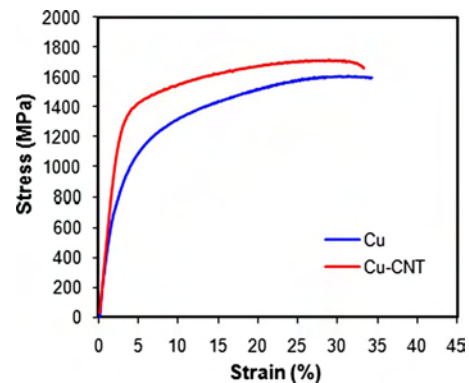


FIG. 4. (Color online) Stress-strain curves of nanostructured Cu and Cu-CNT composite.

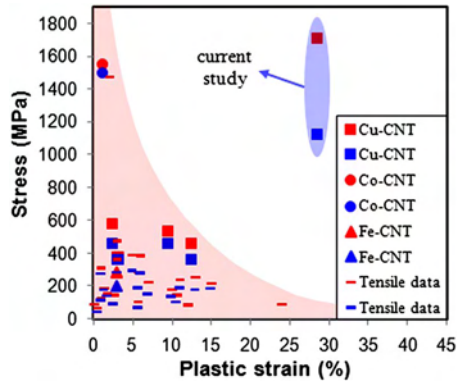


FIG. 5. (Color online) A plot of stress vs compressive plastic strain for metal-CNT composites reported in Refs. 13–16 and current study. The tensile results of metal (Al, AISi, 2024Al, Cu, Mg, Ni, AZ91D)-CNT composites (Refs. 17–27) are also included for reference. Red points: maximum stress; blue points: yield stress.

eral, like nanocrystalline metals,<sup>31</sup> CNT-reinforced metallic composites also show a feature of strength-ductility tradeoff, represented by the shaded red region. In other words, increasing strength is usually accompanied with decreasing ductility. However, the nanostructured Cu-CNT composite fabricated in this study is clearly distinguished from the general trend and out of red region, as seen in Fig. 5. A comparison of the current results with reported data points to a fact that the present Cu-CNT composite has an outstanding improved mechanical performance. In addition, nanoindentation measurement discloses that the presence of CNTs also increased Young's modulus from 91 to 117 GPa, which is consistent with previous results and indicates an increase in stiffness. Furthermore, the area underneath the stress-strain curve, an indicator of energy required to failure, is about 10% larger for Cu-CNT composite than for Cu.

It has been well established that the deformation mechanism depends on grain size and undergoes a transition from dislocation-controlled to grain boundary-mediated characteristics at a critical grain size.<sup>32</sup> When the grain size is below this critical value, deformation behavior is also related to applied strain.<sup>33</sup> As for Cu, the critical grain size is about 10–15 nm.<sup>32</sup> Obviously, the grain size of current Cu-CNT composite ( $\sim 22$  nm) is much larger than the critical value. That is, plastic deformation is mainly controlled by dislocations. However, owing to the fine grain size, the grain interiors are usually devoid of dislocation sources and dislocations nucleate at grain boundaries or CNT-matrix boundaries. Figure 2 has shown that the CNTs can be distributed intra- as well as intergranularly. In both cases, CNTs may be able to inhibit dislocation nucleation and motion, thereby leading to an increase in the yield strength. It is worth pointing out that the grain size refinement caused by CNTs also contributes to the increase in strength of the Cu-CNT composite.

In summary, nanostructured Cu-CNT composite with a grain size of about 22 nm has been produced at room temperature. Microstructure analysis indicates that an addition of 1 wt % multiwalled CNTs can cause grain refinement and narrower grain size distribution. In the Cu matrix, CNTs are distributed both at grain boundaries and in the grain interiors. Moreover, both microscopic and macroscopic characterization suggests that the dispersion of CNTs is homogeneous. Mechanical tests reveal that the nanostructured Cu-CNT composite possesses a combination of high strength and

good ductility. Compared with its counterpart developed under the same condition, an addition of CNTs leads to a considerable increase in strength, stiffness and toughness without a loss in ductility. More importantly, in contrast to the metal-CNT composites reported earlier, the current Cu-CNT nanocomposites exhibit an improved outstanding combination of strength and ductility.

This study was supported by the DOE, Office of Science, Office of Basic Energy Sciences. ZH appreciates the support of Kyushu University P&P program. The authors gratefully acknowledge John Kennison for his assistance in performing powder compaction.

- <sup>1</sup>S. Iijima, *Nature (London)* **354**, 56 (1991).
- <sup>2</sup>M. M. J. Treacy, T. W. Ebbesen, and J. M. Gibson, *Nature (London)* **381**, 678 (1996).
- <sup>3</sup>E. W. Wong, P. E. Sheehan, and C. M. Lieber, *Science* **277**, 1971 (1997).
- <sup>4</sup>P. M. Ajayan, *Chem. Rev. (Washington, D.C.)* **1999**, 1787.
- <sup>5</sup>A. A. Mamedov, N. A. Kotov, M. Prato, D. M. Guldi, J. P. Wicksted, and A. Hirsch, *Nature Mater.* **1**, 190 (2002).
- <sup>6</sup>E. T. Thostenson, Z. F. Ren, and T. W. Chou, *Compos. Sci. Technol.* **61**, 1899 (2001).
- <sup>7</sup>N. P. Padture, *Adv. Mater.* **21**, 1767 (2009).
- <sup>8</sup>P. J. F. Harris, *Int. Mater. Rev.* **49**, 31 (2004).
- <sup>9</sup>C. He, N. Zhao, C. Shi, X. Du, J. Li, H. Li, and Q. Cui, *Adv. Mater.* **19**, 1128 (2007).
- <sup>10</sup>R. George, K. T. Kashyap, R. Rahul, and S. Yamdagni, *Scr. Mater.* **53**, 1159 (2005).
- <sup>11</sup>C. F. Deng, D. Z. Wang, X. X. Zhang, and A. B. Li, *Mater. Sci. Eng., A* **444**, 138 (2007).
- <sup>12</sup>S. R. Dong, J. P. Tu, and X. B. Zhang, *Mater. Sci. Eng., A* **313**, 83 (2001).
- <sup>13</sup>S. I. Cha, K. T. Kim, S. N. Arshad, C. B. Mo, and S. H. Hong, *Adv. Mater.* **17**, 1377 (2005).
- <sup>14</sup>Y. J. Jeong, S. I. Cha, K. T. Kim, K. H. Lee, C. B. Mo, and S. H. Hong, *Small* **3**, 840 (2007).
- <sup>15</sup>K. T. Kim, J. Eckert, S. B. Menzel, T. Gemming, and S. H. Hong, *Appl. Phys. Lett.* **92**, 121901 (2008).
- <sup>16</sup>A. Goyal, D. A. Wiegand, F. J. Owens, and Z. Iqbal, *J. Mater. Res.* **21**, 522 (2006).
- <sup>17</sup>T. Tokunaga, K. Kaneko, and Z. Horita, *Mater. Sci. Eng., A* **490**, 300 (2008).
- <sup>18</sup>R. Pérez-Bustamante, C. D. Gómez-Esparza, I. Estrada-Guel, M. Miki-Yoshida, L. Licea-Jiménez, S. A. Pérez-García, and R. Martínez-Sánchez, *Mater. Sci. Eng., A* **502**, 159 (2009).
- <sup>19</sup>A. M. K. Esawi and M. A. E. Borady, *Compos. Sci. Technol.* **68**, 486 (2008).
- <sup>20</sup>I. Sridhar and K. R. Narayanan, *J. Mater. Sci.* **44**, 1750 (2009).
- <sup>21</sup>T. Kuzumaki, K. Miyazawa, H. Ichinose, and K. Ito, *J. Mater. Res.* **13**, 2445 (1998).
- <sup>22</sup>T. Laha, Y. Chen, D. Lahiri, and A. Agarwal, *Composites, Part A* **40**, 589 (2009).
- <sup>23</sup>C. F. Deng, X. X. Zhang, D. Z. Wang, Q. Lin, and A. B. Li, *Mater. Lett.* **61**, 1725 (2007).
- <sup>24</sup>K. T. Kim, S. I. Cha, S. H. Hong, and S. H. Hong, *Mater. Sci. Eng., A* **430**, 27 (2006).
- <sup>25</sup>E. Carreño-Morelli, J. Yang, E. Couteau, K. Hernadi, J. W. Seo, C. Bonjour, L. Forró, and R. Schaller, *Phys. Status Solidi A* **201**, R53 (2004).
- <sup>26</sup>P. Q. Dai, W. C. Xu, and Q. Y. Huang, *Mater. Sci. Eng., A* **483**, 172 (2008).
- <sup>27</sup>Y. Shimizu, S. Miki, T. Soga, I. Itoh, H. Todoroki, T. Hosono, K. Sakaki, T. Hayashi, Y. A. Kim, M. Endo, S. Morimoto, and A. Koide, *Scr. Mater.* **58**, 267 (2008).
- <sup>28</sup>M. D. Uchic, D. M. Dimiduk, J. N. Florando, and W. D. Nix, *Science* **305**, 986 (2004).
- <sup>29</sup>N. A. Mara, D. Bhattacharyya, P. Dickerson, R. G. Hoagland, and A. Misra, *Appl. Phys. Lett.* **92**, 231901 (2008).
- <sup>30</sup>D. Pan, S. Kuwano, T. Fujita, and M. W. Chen, *Nano Lett.* **7**, 2108 (2007).
- <sup>31</sup>C. C. Koch, *Scr. Mater.* **49**, 657 (2003).
- <sup>32</sup>J. Schiøtz and K. W. Jacobsen, *Science* **301**, 1357 (2003).
- <sup>33</sup>H. Q. Li, H. Choo, Y. Ren, T. A. Saleh, U. Lienert, P. K. Liaw, and F. Ebrahimi, *Phys. Rev. Lett.* **101**, 015502 (2008).